



## **APPENDIX B: Dakota Technologies, Inc. Report on LIF**

*This document was originally issued in support of the LIF investigation of the St. Louis River U.S. Steel superfund site, by the same researcher who developed the LIF technique; and whose company collected LIF at the Minnesota Slip site. Prepared by Randy St. Germain of Dakota Technologies, Inc.; July 2002*

-----

### **In-situ LIF System for PAH Contaminated Sediments**

*Submitted by:*

Randy St. Germain  
Dakota Technologies, Inc.  
2201-A 12<sup>th</sup> St. N.  
Fargo, ND 58102  
Phone: (701) 237-4908  
Fax: (701) 237-4926  
[stgermain@dakotatechnologies.com](mailto:stgermain@dakotatechnologies.com)



## Introduction

Dakota Technologies, Inc. was contracted by URS Corporation (URS) to provide the instrumentation, tools, and expertise needed to remotely measure the laser-induced fluorescence (LIF) of polycyclic aromatic hydrocarbons (PAHs) in lake sediments associated with the USS Duluth Works Site (Site). The effort fell into 5 main categories.

- Measure the fluorescence of previously collected sediment samples (of varying PAH concentration) with the Rapid Optical Screening Tool (ROST). Adjust system parameters to maximize our ability to detect PAHs and distinguish them from naturally occurring interferences.
- Measure and record PAH fluorescence on sediments in real time as the probe was advanced into the sediment.
- Correlate LIF response with sediment samples taken immediately adjacent to the LIF soundings for use in validation/chemometrics analysis studies.
- Submit a report describing the technology and the data generated.

This report documents the effort and is meant to serve as a guide to understanding what was actually being measured, how it was measured, and how the data can and should be interpreted.

## LIF PAH Screening System Description

### *Polycyclic Aromatic Hydrocarbon (PAH) Fluorescence Principles*

#### **Laser-induced fluorescence (LIF)**

Fluorescence spectroscopy is one of the most widely applied spectroscopic techniques in use today. It is, by nature, a fast, sensitive and typically reversible process that makes it ideal for incorporation into a continuous screening technique that uses an optically transparent window as the conduit between the sensor and the analyte. Luminescence is the emission of light from any substance that returns to the ground state after being excited into an electronically excited state. If the bulk of the molecules emit their photons in less than a microsecond the emission is referred to as fluorescence. Emission that takes longer than this is called phosphorescence.

Fluorescence is typically observed in molecules that have an aromatic structure. One class of aromatics is the PAH found in quantity in typical petroleum products. The PAHs found in coal tars, creosotes and even sediments are also fluorescent, but they fluoresce much less efficiently than PAHs dissolved in more solvent-rich environments, such as the aliphatic body that makes up the bulk of fuels/petroleums. We have observed that the less solvent available, the less efficiently the PAHs fluoresce. The PAHs continue to absorb the excitation light, but there is a much higher likelihood of the PAHs finding a non-radiative mechanism with which to shed the additional energy they picked up during the absorption of the excitation photon(s). In spite of this, the PAHs in sediments can still be coaxed into fluorescing well enough to allow in-situ laser-induced fluorescence screening via a sapphire-windowed probe.



A plot of the relative distribution of the different colors (or energies) of the photons being emitted by an excited sample of PAH is called the spectrum (or spectra when referring to more than one). Figure 1 illustrates the concept of PAH absorbance and fluorescence spectra. The spectra of individual PAH species (such as naphthalene and anthracene) can contain enough structure (peaks and valleys) to be identified in simple mixtures in the lab. The fluorescence of PAHs in sediments however, is originating from such a wide variety and concentrations of PAHs and differing local environments (dissolved phase, sorbed to particles, microcrystals, etc.) that the resulting spectra are very broad and contain very little "structure" that one might use to determine which individual PAHs are responsible for the fluorescence. The spectra do shift enough to recognize that the distribution of species or environments are changing, but individual speciation is impossible.

Another property of fluorescence that can be measured is the varying amount of time it takes for the molecules to emit the photons after exposure to a pulsed excitation source, such as a laser is illustrated in Figure 2. If we use a time sensitive detector to observe the number of photons being emitted over time, we can derive more information about the nature of the fluorophores and their environment. This decay time information contained within the waveform is measured with an oscilloscope. The different PAHs and the differing environments that exist in sediments all combine to change the decay times observed. This information is readily obtained when using a pulsed source such as the laser we used in this application. Our apparatus (described in the [ROST System Description](#) section) allows us to investigate not only what colors are being emitted, but also how long it takes for the excited population of PAHs to emit the fluorescence photons. We use a patented method of combining the photons from four regions of the emission spectrum optically collected over 20 nm wide sections of the emission spectra at 340, 390, 440, and 490 nm.

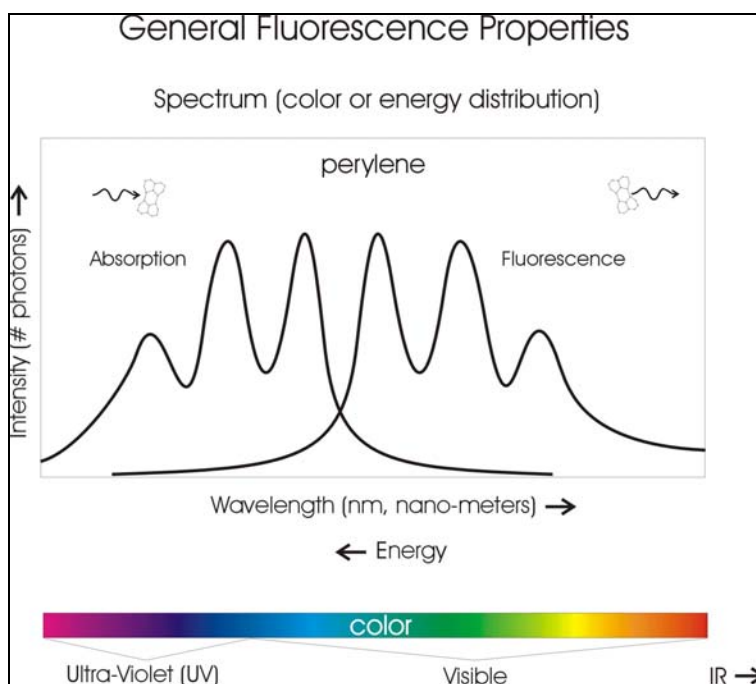


Figure 1. Spectral property of fluorescence

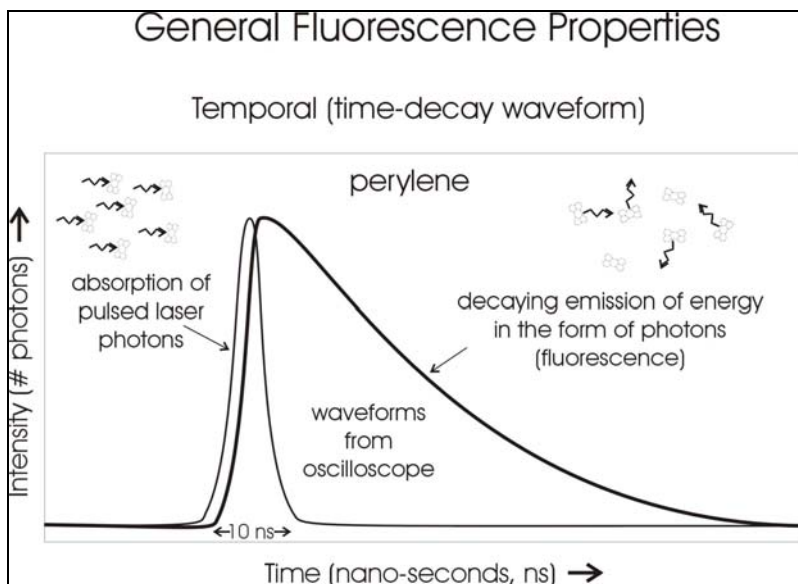


Figure2. Temporal property of fluorescence

These four "channels" are delayed in time through successively longer fiber optic delay lines and eventually arrive at the detector (photomultiplier tube or PMT). The resulting oscilloscope waveform is a unique measurement of both the spectral and temporal components of the fluorescence. This allows us to simultaneously observe the spectral and temporal qualities of the fluorescence. This technique is described in detail later in this report. It is these multi-wavelength waveforms, measured continuously and stored vs. depth, that ultimately serve as our indicator of PAH concentration vs. depth in the sediment.

## Interferences

Nature has co-deposited a myriad of additional fluorescent materials in sediments that will also absorb the laser light and fluoresce intensely enough to complicate the measurement of the PAH fluorescence. Example materials include minerals such as calcites and a variety of biological materials. Both living organisms and their associated breakdown products (humic and fulvic acids) fluoresce well enough to interfere with the observation of the fluorescence of the target PAHs. This fluorescence, along with scattered excitation laser light and Raman light generated throughout the optical train (fiber optics) will ultimately make it back to the detector, mixed in with true PAH fluorescence, and must be accounted for in some fashion. Throughout this document we will refer to all these sources of non-PAH emitted photons as "background" fluorescence, even though the true source might well be non-fluorescent (scatter) in nature.



## Understanding ROST Fluorescence Waveforms

Spectroscopic techniques involve probing the target matrix with light and learning about the contents of that matrix by analyzing the light that is emitted or absorbed by the target matrix. For screening tools it is crucial to glean as much information from this light as one can in as little time as possible. ROST accomplishes this task in a novel fashion. The fluorescence data from ROST is deceptively simple. There is a lot more going on in a ROST waveform than one would imagine at first glance. It is actually a two-dimensional data set that contains three-dimensional fluorescence information. To complicate this, some of the information is overlapping. A full description of the multi-wavelength waveform data follows in order to give the reader an understanding of the data acquired during this study.

### ***PAH time decay waveforms***

Each type of PAH molecule (such as phenanthrene, naphthalene, or anthracene) emits fluorescence over a unique time period after being excited by a pulsed excitation source such as the laser used in ROST. The emission starts out at maximum intensity, and then decays away at a rate unique to each type of PAH. The number of rings, the bonding between them, the amount of substitution on the rings, and other structural features of the molecule determine, to a great extent, the decay rate exhibited by a particular PAH. One class of molecule, the PCBs, have a structure that would seem to fluoresce well, but the chlorine substitution on the rings causes what is referred to as the heavy-atom effect, resulting in non-radiative relaxation from the excited state and a dramatic reduction in fluorescence. In fact the reduction is so significant that PCBs are essentially non-fluorescent molecules.

The environment in which the PAH exists also has a substantial influence on the decay rate. Quenching, which refers to any process that causes a decrease in the decay time (as well as the intensity) of the fluorescence, is dependent on conditions like oxygen levels, solvent availability, solvent viscosity, and a myriad of other matrix dependent conditions. An example of this can be found with the fluorescence of PAHs in fuels (gasoline, diesel, or kerosene) vs. coal tar oil. The coal tar oil can often contain more PAHs than the fuels, but the fluorescence lifetime is much shorter and the total fluorescence of fuels is often 2 to 3 orders of magnitude more intense. If one were to dissolve coal tar in a solvent such as hexane, its fluorescence intensity would rival that of fuels because the solvent matrix is simply more suited to allow fluorescence to occur.

Figure 3 illustrates the differing decay times one might observe for 4 different PAHs, along with the time profile of the laser pulse that excited them. Now remember, these are large populations of PAHs being excited and while some begin emitting immediately, other individual PAH molecules "wait" many nanoseconds before emitting a photon. What is plotted here is a picture of the distribution of times that the PAHs are remaining in the excited state before emitting photons. Now in our case (sediments) we have many different PAHs of differing ring number and substitution levels. The bold curve in Figure 3 illustrates the fluorescence decay profile that would result if we observed the fluorescence of all four PAHs simultaneously. This is the fluorescence waveform that would result if all 4 different PAHs fluoresced with equal intensity (normalized to keep it on scale). This same concept is happening in the sediments. We are observing the sum of all the decay profiles for all the different PAHs that are absorbing and



emitting photons with each pulse of the excitation laser. It should be noted that there is no predictable trend between decay rate and structure like the trend that exists between spectrum and structure as described below.

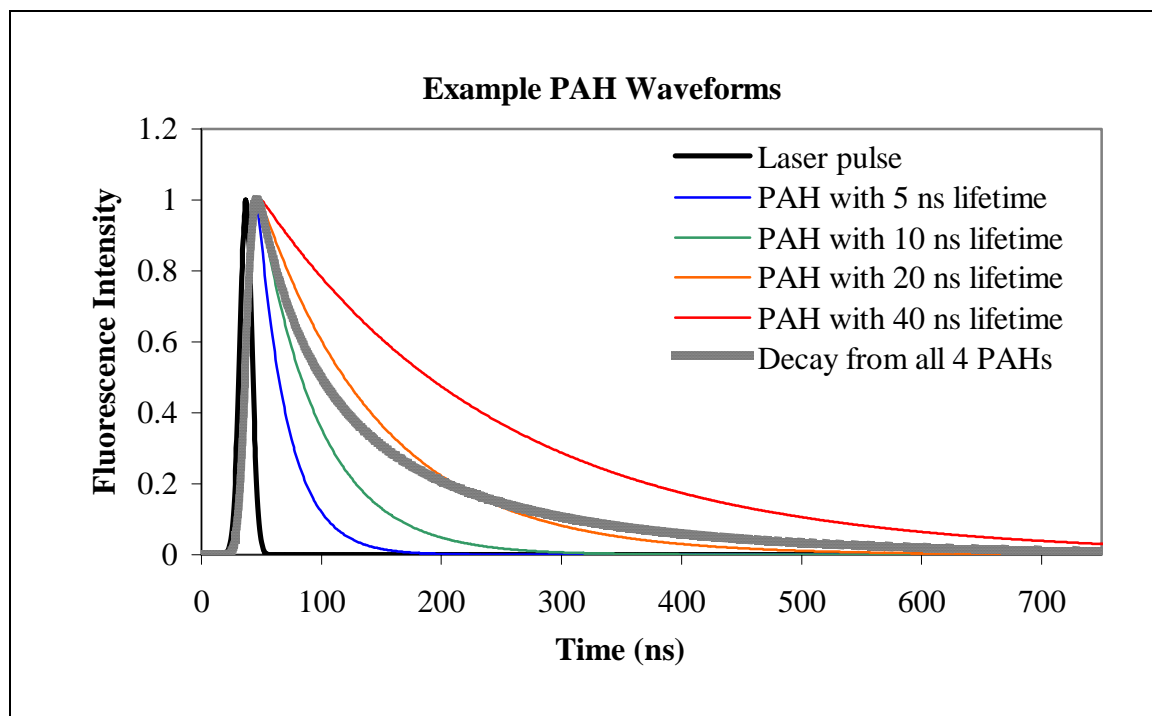


Figure 3. Temporal fluorescence examples

Of course the fluorescence decay profile observed in sediments is not made up of equal amounts of fluorescence from the various PAHs found in them. The wavelengths of light being emitted by (spectra) and the relative fluorescence yields of the different PAHs are all quite different, but the concept is still valid. The decay profile of the PAHs observed in the sediment results from the decay profiles of a mixture of different PAHs, along with fluorescence from other materials in the matrix.

### **PAH spectra**

Let's take a look at the other property of the fluorescence emission of the same 4 example PAHs we showed at in Figure 3. This time we'll examine not the time over which they fluoresce, but instead the distribution of energies found in the photons they emit. Remember that the fluorescence emission spectrum of a pure PAH is simply a graphical representation of the energy distribution of photons that are emitted from a large population of the PAHs as they release energy that was absorbed from the excitation beam of light (in our case, a laser). Spectra of pure PAHs are typically acquired by dissolving a sample of the pure PAH in a pure solvent that does not fluoresce.

Figure 4 depicts the fluorescence emission spectra of the same 4 PAHs used in the temporal example in Figure 3. The laser wavelength is also shown in Figure 4, demonstrating the principle that fluorescence occurs at longer wavelength (lower energy) than the excitation wavelength (also known as Stokes' shift). The basic trend is toward longer wavelength emission



as more rings are added or substitution increases. Naphthalene emits at around 340 nm and the spectra "red-shift" as the number of rings increase. Another general property of fluorescence is that for a pure PAH the emission spectrum remains the same irrespective of what wavelength of light is used to excite them (Kasha's rule). This is not true for mixtures however, because changing the excitation wavelength might well change which PAH are being excited and to what degree. The bold spectrum in Figure 4 is the combined spectra of all 4 PAHs. This is a simplified illustration of what generally happens if we observe the total fluorescence of a mixture of different PAHs. Any change in the relative amounts of the differing PAHs or changes in the matrix in which they exist will cause a change in the spectrum of light actually emitted.

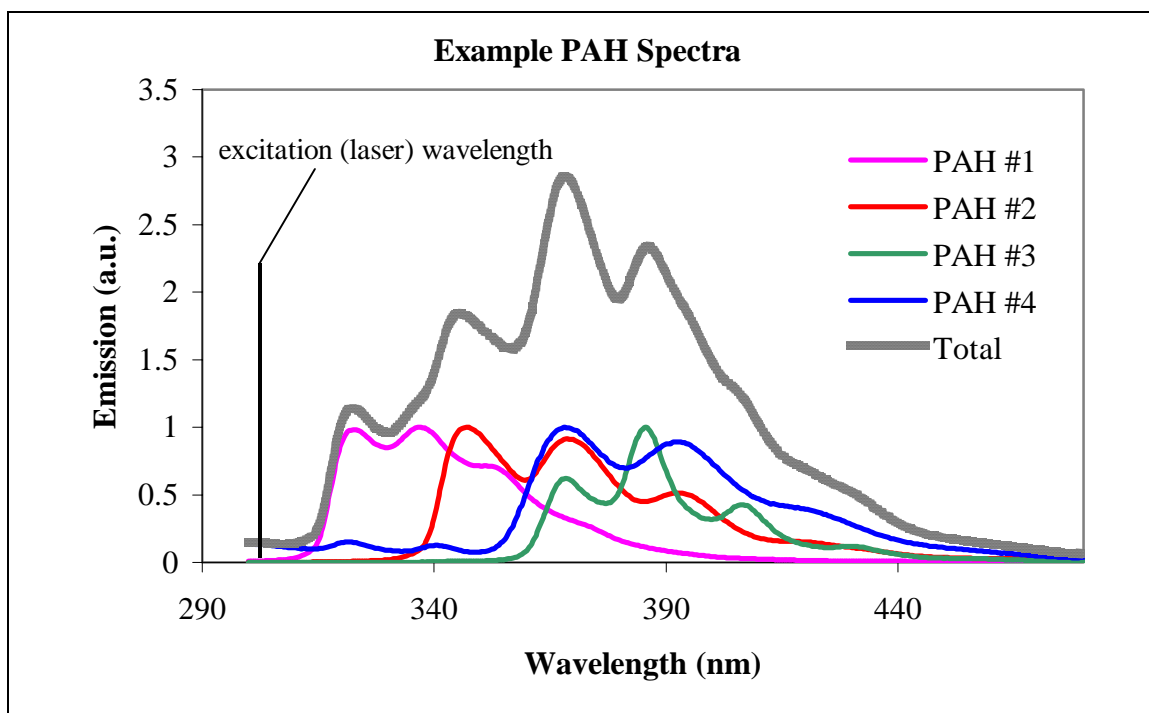


Figure 4. Spectral fluorescence examples

The fairly well defined structure (multiple peaks, valleys, and their various positions) of the spectra in Figure 4 suggests that perhaps one could use algorithms to extract information about the relative concentrations of the individual PAHs. While this is possible for very simple mixtures (2 to 3 PAHs) under controlled conditions, the algorithms quickly fail when many PAHs are present and interference fluorescence from humics, fulvics, and minerals is introduced. At best, one is able to use the overall shape of the total fluorescence spectrum to predict the *type* of mixture (diesel, coal tar, crude oil, etc.) and, in fact, this is routinely accomplished in environmental fluorescence forensics.

### **PAH multi-wavelength waveform (MWW)**

The fluorescence of PAHs has both a spectral and temporal component. Real-world environmental samples typically contain at least several (if not dozens) of different PAHs along with other fluorophores, and the PAH fluorescence spectra overlap to form broad and fairly featureless spectral and temporal emission (compared to pure PAH spectra). If we were to record the temporal decay waveforms across the entire spectrum we would record what is called a wavelength-time matrix (WTM) that would describe the fluorescence emission completely. To



create this we scan the emission selection monochromator from wavelength to wavelength, monitoring the pulsed emission vs. time at each wavelength with an oscilloscope.

Figure 5 contains the WTMs of diesel, jet, creosote, and gasoline on sand at several thousand ppm. The difference between the contaminants is clear and identification is straightforward. Dakota Technologies, Inc. (DTI) once employed these matrix style data sets to completely analyze the fluorescence of petroleum, oil, and lubricant (POL) contaminated soils. WTMs were (and still are) excellent for identifying/classifying the PAH fluorescence of environmental samples because of the unique information that both dimensions of PAH fluorescence exhibit when acquired in unison. While WTMs make different contaminants readily discernable from one another, they are 3-dimensional and large. Also, the screening tool must be held still while the measurement is being made. All of these qualities make WTMs unwieldy for environmental screening tools that are designed to continuously log (typically 1 Hz) the presence of PAHs vs. time or depth.

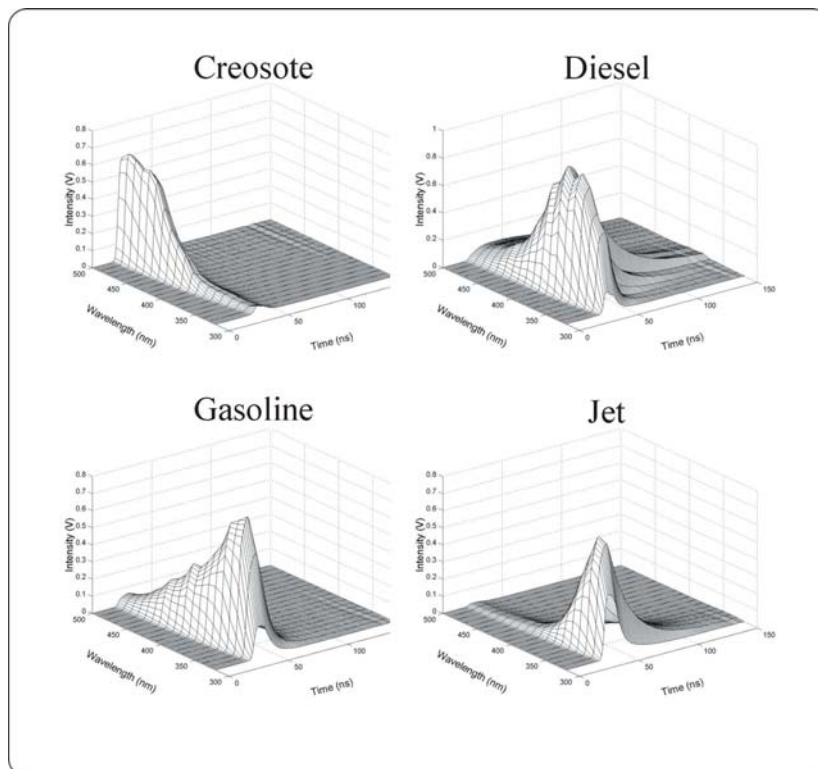


Figure 5. Example WTMs of common contaminants on sand

Because WTMs are so difficult to implement in screening mode, DTI developed (and patented) a multiple-wavelength waveform (MWW) technique that allows multi-dimensional PAH fluorescence measurements to be acquired "on the fly". Figure 6 illustrates the concept. Select regions of the spectrum are monitored for their temporal response. The responses are optically delayed and recombined, and the resulting responses converge to form one two-dimensional waveform. There is sometimes overlap between the "channels" with long decay times, and the spectral regions being monitored are fewer and farther between than WTMs, but the resulting waveform still retains a unique combination of spectral and temporal fluorescence information that makes speciation and identification of PAH mixtures possible. Figure 7 illustrates the



unique waveform produced by a variety of common PAH-containing environmental contaminants.

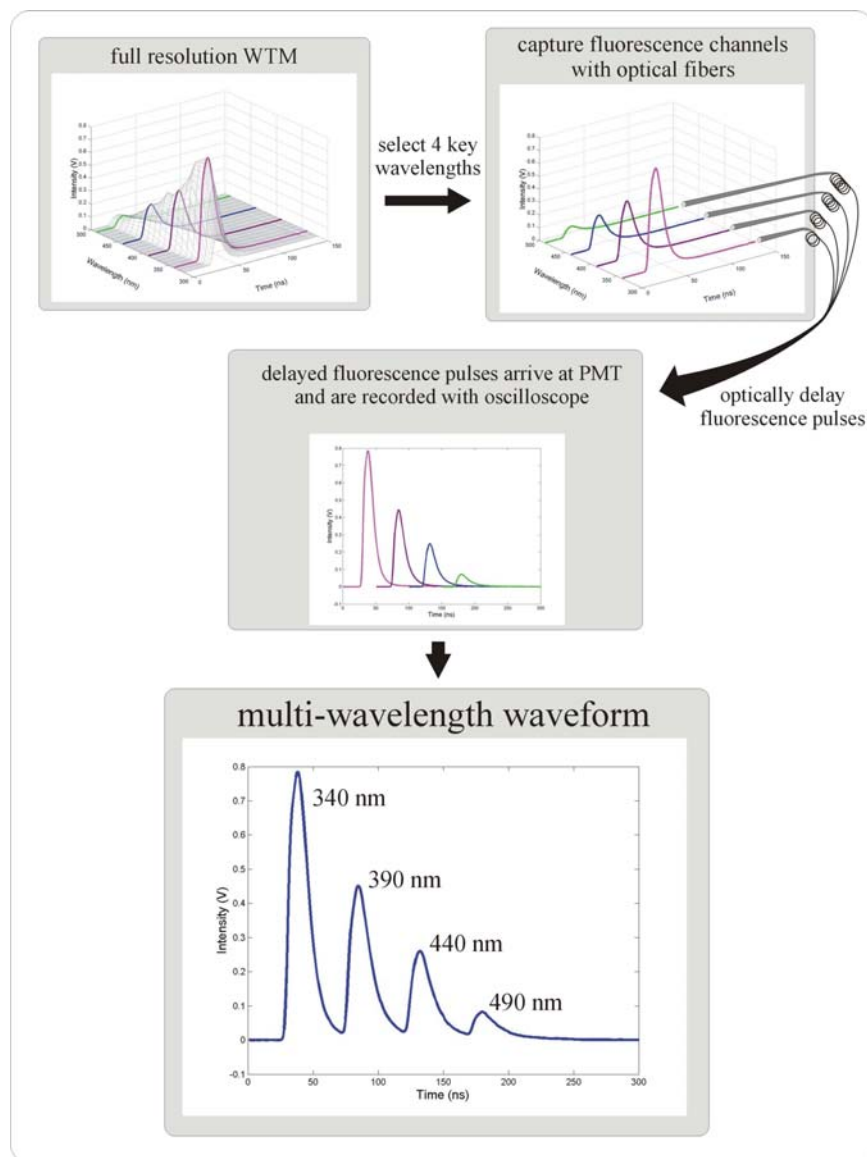


Figure 6. Multi-wavelength waveform concept

The ROST system acquires waveforms at ~1 Hz and logs them to the hard drive continuously. As described below (see [Calibration and normalization](#)) the waveforms are integrated to achieve a quantitative result that is plotted vs. depth. The shape of the waveform yields information on the nature of the fluorescing material. With experience the analyst learns to look for changes or similarities in the waveform and is able to assess changes in the analyte concentration or the matrix. For instance, are the decay times for the various channels changing due to changes in the PAHs or perhaps changes in oxygen levels that affect quenching? Is the emission shifting to shorter or longer wavelengths due to changes in the amount of degradation via biological activity, weathering, or volatilization? Is the first channel (closest to the laser) getting more or less contribution from laser scatter due to improper mirror alignment? These and a myriad of



other questions and answers can be gleaned from the shape of this simple, yet informative, data format.

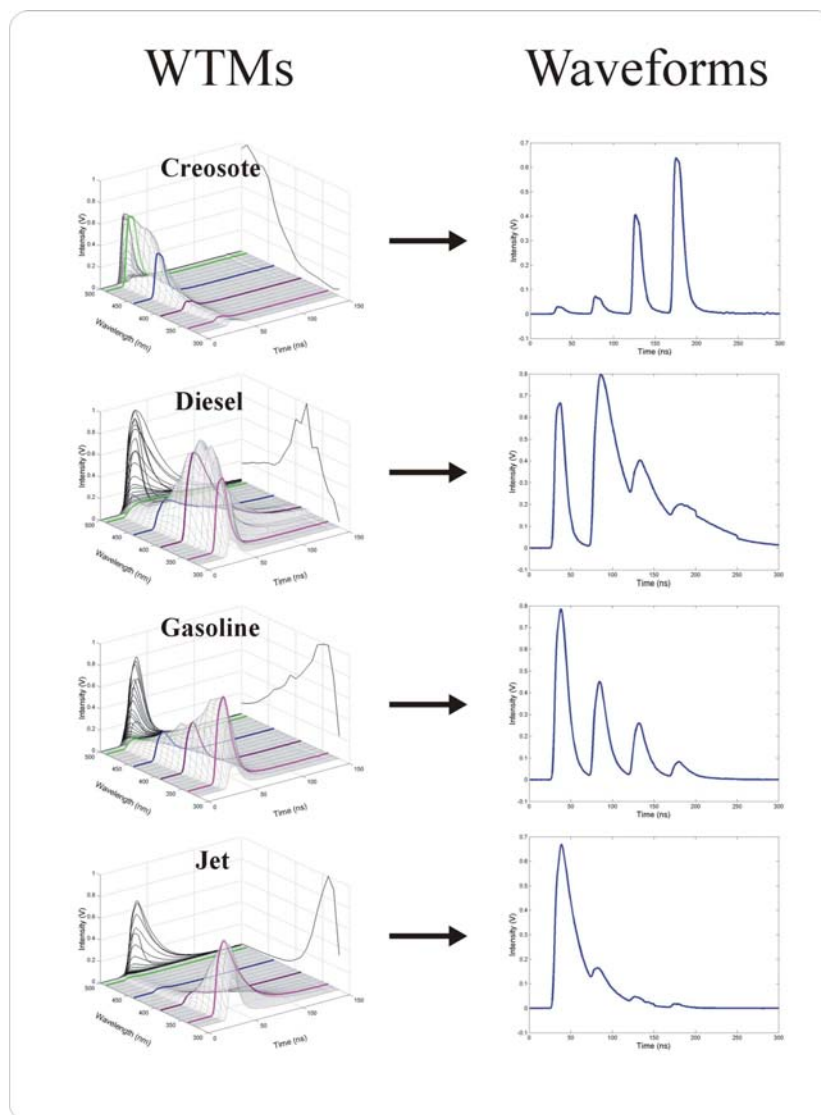


Figure 7. Waveforms of common contaminants

### ***FVD colorization***

The waveforms that are continuously logged vs. depth with ROST contain a wealth of information, but to make this information easily interpretable in fluorescence vs. depth (FVD) log format, we need to further reduce the data to a one-dimensional data set that we can plot vs. depth. As discussed, the quantitative information is contained within the area under the waveform (total fluorescence) but how do we convert a waveform's shape into a singular entity? To accomplish this, DTI has developed and implemented a novel technique that effectively converts the shape of the waveforms into colors. These colors are then used to fill in the area under the FVD that represents the total fluorescence measured at each point in the FVD. Figure



8, derived from data from a coal tar delineation project, illustrates the technique of colorizing the FVD according to the shape of the waveforms.

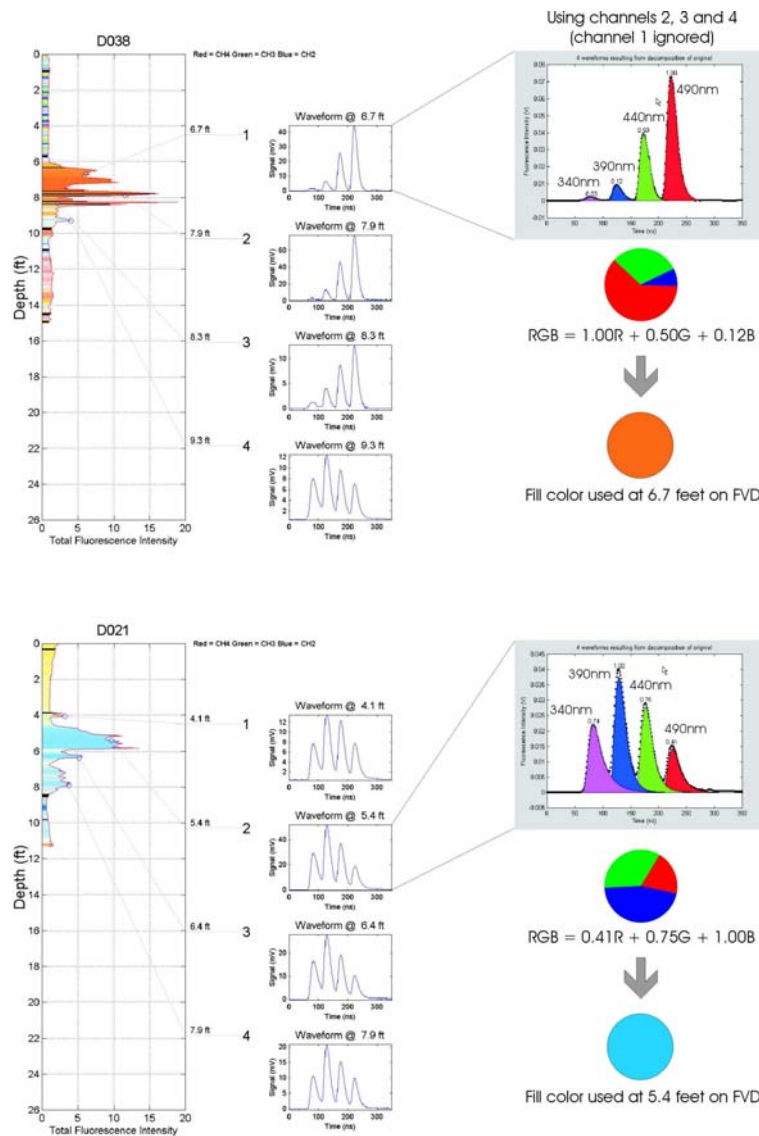


Figure 8. How color-coding is calculated

The result is a data presentation technique that allows the user to assess similarities or changes in the waveform shapes vs. depth by simply observing the colors that represent the shape of each and every waveform in the data set. This technique was used on the sediment measurements made in this project, both in the lab and in the field. It should be noted that the color black indicates that the algorithm that calculates the color failed to deconvolve the waveform successfully.

The colorization technique is limited to using three of the channels as a result of the red, green, and blue (RGB) color definition which computer colorization systems typically implement. A cyan, yellow, magenta, and black colorization system (CYMK) might allow the use of all four channels and is currently being considered as a replacement for RGB. The first three channels



(340, 390, and 440 nm) were used to colorize the data in this study. The 490 nm channel was used in a quantitative sense, but was ignored for the colorization. It should be noted that a strictly temporal change (where only the decay times change, not the spectrum) would not necessarily result in a color change, since the ratios of the 3 channels used might remain constant even though the area under the waveform itself will increase or decrease.

An added benefit of this technique is that it provides insight in situations where non-linear response behavior is encountered. Many contaminants such as coal tars, heavy crudes, and creosotes do not fluoresce with concentration in a linear fashion. For instance, a 10 fold increase in PAH concentration might produce very little or no increase in total fluorescence intensity. However, a spectral or temporal shift often does continue to occur with changes in concentration due to energy transfer, photon cycling, and other phenomenon. The color of the FVD fill continues to darken or shift in color, acting as an indicator of a change in the fluorescence of the sample, alerting the analyst to a possible increase in concentration. While this technique is less than analytical it does provide the analyst with additional insight into the distribution of PAHs in the soil vs. depth.

## ROST System Description

The ROST system is contained in a ruggedized shipping container as shown in Figure 9. The system actually consists of a variety of sub-systems that are described in detail in this section.

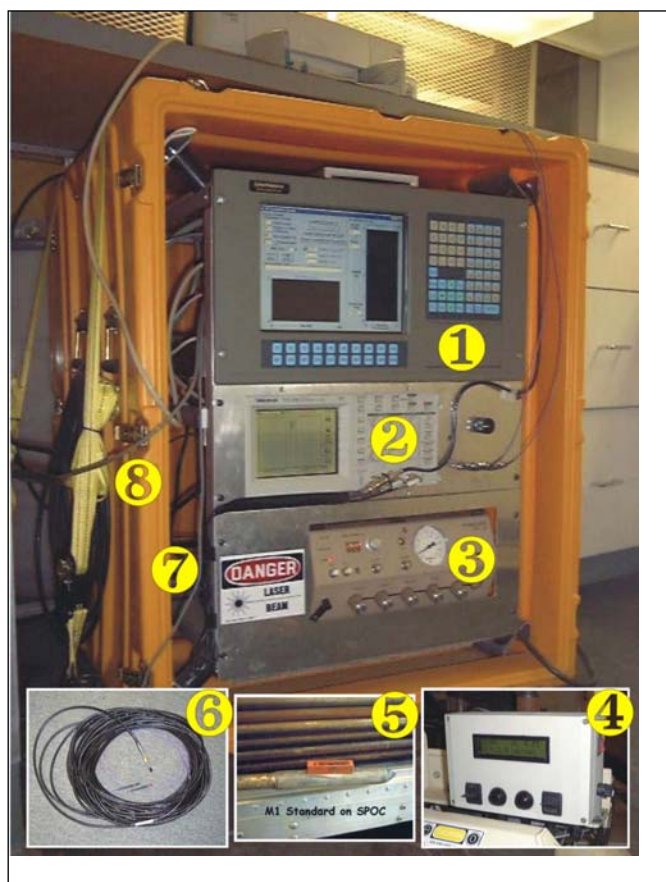


Figure 9. ROST system and key peripheral devices



## Laser ☐

The ROST system employs a pulsed XeCl excimer laser (MPB PSX-100) that generates very fast pulses of 308 nm light at 50 Hz. Each pulse measures less than 10 billionths (10 ns) of a second wide at half height. The 308 nm wavelength efficiently excites the vast majority of PAHs that are contained within the sediments being screened. A beamsplitter directs a small portion of the beam to an energy meter to monitor excitation pulse energy. A photodiode is positioned near the beamsplitter and serves as the trigger source for the time-resolved fluorescence measurement that takes place with the oscilloscope. A lens is used to launch the laser light into a fiber optic for delivery to the subsurface.

## Fiber optic cable ☒

The fiber optic cable consists of two 40 m silica/silica optical fibers. One fiber delivers the excitation pulse while the other serves to return a portion of the resulting fluorescence to the surface for measurement. Both silica/silica fibers with a 365 micron core-diameter and are SMA terminated at the surface. The fibers are terminated with a custom connector at the sub-surface (SPOC below). Since the fibers are readily broken if flexed or handled too aggressively, they are housed in a flexible polyurethane covered stainless steel sheath with bend radius limiting quality that drastically reduces fiber optic failure rates.

## Shock-protected optical compartment (SPOC) ☐

The fiber optics deliver and receive the light to and from a steel probe that consists of 2 threaded Geoprobe<sup>®</sup> rods (1 inch diameter) terminated with a special optics module and tip called a SPOC. DTI typically uses a Geoprobe to jackhammer the LIF probe into the sub-surface to delineate typical POL spills, such as leaking underground storage tanks. Fibers terminated into a standard optical mount would shatter or cleave instantly under the shock and vibration of the jackhammer. DTI developed and built the SPOC that employs proprietary elastomer supports, in combination with Swagelock fittings, to insure long term stability of the optical alignment along with protection against breakage. The SPOC contains a parabolic mirror that acts to turn the excitation beam 90 degrees. The beam exits the SPOC through a sapphire window that is flush-mounted on the side of the SPOC and strikes the sediment that is pressed against the window as the probe advances through the sediment. Sapphire's Moh hardness of 9 (2<sup>nd</sup> in hardness only to diamond) allows it to resist scratching or breaking under all but the most severe conditions such as jackhammering into gravels/cobbles. The laser beam illuminates several mm<sup>2</sup> of the sediment that is exposed to the window's surface and any resulting fluorescence (along with a substantial quantity of scattered laser light) is emitted back into the window where a portion is reflected by the parabolic mirror into the return fiber for transport to the surface.

The SPOC design is watertight; a necessary attribute when probing in saturated zones such as those obviously experienced when probing sediments. Any leakage can result in evaporation of the intruding water into the air space within the SPOC. The water vapor that results can cause fogging on the interior surface of the sapphire window that has the effect of changing background levels and reducing fluorescence intensity. The moisture can also cause corrosion of the optics and hardware within the SPOC. An extra measure of humidity prevention is achieved by purging the SPOC with an inert gas immediately prior to reassembly any time it is open to the atmosphere for maintenance or adjustment.



## Emission detection system $\angle \nabla$ (hidden from view)

The collection fiber returns the entire spectrum of light ("white light") that is collected from the sediment surface. Since this is a multi-channel (multi-wavelength) detection system, we must disperse the white light. To accomplish this, the collection fiber is butt-coupled directly into an Acton SP150 imaging monochromator where a series of mirrors and a 600 groove/mm grating act to disperse the white light into a "rainbow" that can be sampled (4 regions at 340, 390, 440, and 490 nm) for detection.

Before the light is dispersed by the monochromator the laser light (308 nm) must be removed and the amount of fluorescence light must be controlled. If not rejected, the relatively intense laser light that accompanies the fluorescence bounces around the interior surfaces of the monochromator and ultimately ends up in the detector. The detector does not differentiate between laser light and fluorescence, so this laser light must be filtered out. To achieve this, a cutoff long-pass filter (320 nm CFLP) is arranged immediately inside the monochromator, rejecting the vast majority of laser light, but passing the lower energy (longer wavelength) fluorescence. Butt-coupling of the fiber to the monochromator eliminates the slits that are usually found on the entrance of a monochromator. These slits are designed to control bandpass and the amount of light that enters the monochromator to avoid saturating the detector. The ROST system employs a neutral density filter wheel for controlling light levels instead. By selecting an appropriate optical density filter the light levels can be controlled with precision. The reference emitter signal (M1 described later) was attenuated in these studies while the PAH fluorescence was passed through without filtering due to its relatively low intensity compared to standard POLs.

The fluorescence passes through the CFLP and neutral density filterwheel assembly and is ultimately dispersed into a rainbow of light on the back plate of the monochromator. The polished faces of 4 fiber optics are located on this plate and are arranged to "pick off" 4 regions of the spectrum where PAHs fluoresce with varying intensity, depending on number of rings and substitution level of the PAHs being observed. Rotating the grating allows selection of different regions, but always with 50 nm between channels because the space between fibers is not adjustable. ROST uses 340, 390, 440, and 490 nm under standard conditions and these wavelengths were used here.

At this point if all four fiber optics were of the same length and were directed into the detector (PMT), we would observe all four channels combined into a single decay curve (waveform). To achieve separation of the four channels we must time delay the photons so that they strike the detector at different times. To achieve this the fiber optics are all made 10 m longer than the next. The fibers are 2, 12, 22, and 32 m long for the 340, 390, 440, and 490 nm wavelengths, successively, delaying each channel by approximately 50 ns. These four fibers are then terminated in a single large core SMA fitting which couples to a large diameter (1500 micron) fiber optic that is .33 m in length. This large diameter fiber is taken through a relatively sharp bend that serves to "mix" the 4 fiber optic beams into one homogeneous beam. The large fiber is attached to a mount that directs the light at the photocathode of the PMT detector.

The dynode chain of the PMT is held at a -900 V bias with a high voltage power supply. This bias accelerates and multiplies the electrons that are ejected from the photocathode when the photons strike the surface. The PMT detector (Hamamatsu R928) essentially converts the pulse



of photons into a pulse of electrical current. The pulse is actually a train of 4 pulses that results from each channel's photons arriving at the PMT in succession.

### **Oscilloscope $\not\subseteq$**

The pulse of electrical current is very short lived. In fact, the entire train of pulses (the waveform) arrives in less than 250 ns. A very fast device is required to accurately record the current pulse. The ROST system employs a 100 MHz Tektronix® TDS 220 digital storage oscilloscope capable of 1 billion samples per second (1 GS) to record the waveforms. A 50-ohm terminator at the input of the fluorescence channel converts the current to a voltage, allowing measurement of a voltage vs. time waveform that represents the arrival of the photons at the PMT. A second channel of the oscilloscope is used to monitor an energy meter (a much slower measurement) before each test, to log the laser energy performance for maintenance/service tracking purposes. The fluorescence waveforms are displayed on the oscilloscope in real time and are retrieved from the oscilloscope via general-purpose interface bus (GPIB) for storage and analysis. Approximately 50 laser shots are averaged for each sampling point along the test, which ends up being equivalent to a 1 Hz waveform storage rate. At the probe advancement speed used in these studies, the vertical data density averaged 0.3 to 0.5 inches (0.8 to 1.0 cm).

### **Control computer $\supseteq$**

A rack-mounted industrial computer is used to control the ROST system and log the data to hard drive. The computer controls the monochromator, the oscilloscope, a differential GPS beacon, and the depth control and acquisition module (DCAM). The host computer program was written in Visual Basic 5. The software provides a real time display of the test results while the test is in progress and generates a full color picture of the log at the end of the test. The waveforms are continuously logged to the hard drive while a total FVD log is created by integrating the entire fluorescence waveform and plotting it's intensity vs. depth. The final data analysis and display was done on a separate workstation in the office.

### **DCAM $\subseteq$**

During an Air Force SBIR Phase II project, DTI designed and built the original DCAM. It allows a host computer to track and control the probe advancement on a Geoprobe platform. DTI built and delivered a modified version of the DCAM that monitored the gear/proximity sensor on the derrick, displayed the current depth, and communicated the results to the ROST host computer via RS-232 commands for this project. The system runs off 12 V which was supplied by the Geoprobe track rig.

### **Calibration and normalization**

The ROST system response depends on a host of factors. These include laser energy, fiber termination quality, neutral density filter selection, parabolic mirror efficiency, and fiber length, just to name a few. To account for changes in these over time and location, a single point calibration and system check is performed. A reference emitter (coined M1) is placed on the sapphire window and the response is measured. The M1 solution is permanently stored in a quartz cuvette for convenience and the measurement takes place through the wall of the cuvette. This proprietary mix of hydrocarbons fluoresces efficiently across the entire system and serves as both an indicator of system function and as a data normalization benchmark.



The total fluorescence intensity (area under the waveform) of M1 serves to normalize the data from the push that immediately follows the reference emitter measurement. All the FVD logs are presented as a percentage of the signal achieved with M1. The area under every waveform in the data set is integrated, resulting in a pico-Volt-seconds unit (picoseconds \* V or pVs). These values are divided by the pVs measured for M1, and the result is multiplied by 100. The result is a log with x-axis units of percent of M1. This creates a normalized data set that takes into account the entire system performance, from end to end (laser to oscilloscope). The shape of the M1 waveform acts to guide the operator in assessing proper alignment of the detection system. The relative contribution for each channel and the shape of M1 waveform is monitored for consistency to insure that the waveforms remain consistent from day to day.

The DCAM monitors an optical encoder on a Geoprobe direct push probe advancement system. The DCAM's sole function is to monitor the proximity sensor, calculate the speed, direction, and distance traveled, display the result on a digital display, and make the results available to the ROST computer via RS-232 protocol.

## **Field Work Description**

Given the proposed use of this technique on ice, two Geoprobe direct push probe advancement systems were mobilized to the site; a standard truck mounted system and a lighter (but slower moving) skid steer vehicle. The ROST system, housed in its rugged container, was transferred to the skid-steer vehicle once most of the sample locations with sufficient ice to support the truck's weight were obtained.

DTI performed LIF and Geoprobe investigation services at the site from March X to March Y, 2002. A URS field geologist directed DTI efforts with respect to selected sample locations, boring depths and sediment core locations.

## **LIF Waveform Analysis**

DTI has written software that allows us to extract information from the raw waveforms in a continuous fashion along the entire FVD log. This permits classifying certain waveform shapes as belonging to certain contaminant or naturally occurring fluorophore classes. URS's field observations and validation sampling information was used by the analyst at DTI to generate a Basis Set of waveforms that represent the general classes of waveforms observed at the site. Every data point in an FVD log has a complete waveform associated with it. The previously determined Basis Set of waveforms was applied to each of the raw waveforms using a non-negative least squares fit algorithm. An automated software system calculated the relative contributions of each class of waveform for the entire FVD log. The result of the analysis was a measure of how much tar, peat, and system/soil background is represented within the raw logs. An ASCII file and JPG image of the resulting individual component contribution logs were produced and supplied to the URS. The analysis results are valuable for understanding the distribution of the contaminants and natural interferences identified earlier during the Basis Set determination.



**Brief summary of the Analysis:**

1. The raw FVD ACSII data files and colorized JPG images of the plotted logs of each boring were provided to URS. URS provided detailed sediment characterizations/observations and analytical results that identified boring locations and depth intervals that were associated with sediment types of interest (i.e. non-native “coal tar” sediments and native peat).
2. The LIF logs were loaded into the analysis software and several color-coding schemes were examined. I decided that assigning the color rendition to 440nm(Red), 390nm(Green) and 340nm(Blue) RGB color scheme gave best contrast between product types (after reviewing preview images). These were the same channels used in the field and other combinations didn’t result in improved differentiation (contrast) between tars and peat.
3. I harvested (with depth cursors in software) 3 types of tar signals that I kept running across when I reviewed printouts of the logs and the spreadsheets and other documentation URS supplied us with. The tars gave consistently longer decay times (wider peaks) than the peats, but the intensity distribution in the last 3 channels seemed to shift spectrally. This could be a result of differences in oxygen content, soil type, or even tar type. Nonetheless, historical experience and URS filed observations supported the theory that all these types of waveforms were tars. I decided that if I chose tars that covered the entire range of left-right shifting, the algorithm would be able to match any tars it came across by using some combination of the 3 tars of the basis set. (see SaveTar\*. \* images to understand where the tar Basis Set waveforms were harvested from)
4. I harvested two peat signals that seemed to represent the two major classes of peat that I observed in the data set when reviewed against the documentation provided by URS. The peats consistently yielded very short lifetimes (very narrow peaks in time shown in waveform plots). Again, I felt that the non-negative least squares fit algorithm would be able to match all the peats found in the data set by using some combination of the two peat Basis Set waveforms. (see SavePeat\*. \* images to understand where the peat basis waveforms were harvested from).
5. I loaded each FVD, selected a background region (lowest signal) to use as the Background waveform of the Basis Set, and then ran the automated routine that looks at each raw waveform and attempts to fit the raw with some combination of the Basis Set. The ‘Setup’ names (JPGs and PNGs) represent the data just before analysis and the ‘Result’ names show the results of the analysis. The last column shows the residual between the best fit and the raw data.

Area vs. depth (.AVD) ASCII files that contain the results of the analysis were supplied to URS. The ‘parsed’ file contains the ASCII data of what was displayed in the ‘Result’ images. The columns contain Depth, Raw, TarTypeA, TarTypeB, TarTypeC, PeatA, PeatB, and residual data, respectively. The other .AVD files for each log contain the depth and fluorescence area for each basis waveform’s individual contribution. Tar and peat distribution can now readily be



introduced into GIS plotting programs by simply totaling the tar components or peat components vs. depth. DTI could provide this service at a nominal fee if desired. Any output data format, any combination of channels added, averaging over depth intervals (summing or averaging over 6 inch averages, correcting for water depth automatically to give elevation tagging, etc.) could be accommodated since we have programs capable of doing these tasks for large groups of files automatically.

Overall I was pleased with the consistency of the analysis results vs. field observations. Many of the logs showed very consistent transitions between tar types and separation between tars and peats. There were some logs that showed some unique patterns and these were repeated across a number of locations. Some of the logs show a consistent “melding” of both peat and tar signals, with the distribution “oscillating” back and forth. Examples include G30, G34, and I30. I suspect that these logs might be a unique material or condition. Further validation might determine that this is co-mingled tar and peat, a new tar type, or new peat mineral type. Re-running the data wouldn't be necessary though. If additional validation sheds insight and a certain material is identified as being responsible, the oscillatory behavior itself, or the ratio of peat/tars to each other could be used as the ‘indicator’ for that unique material.

Examination of the analysis results often triggers a deeper understanding of the situation. Many clients have had “eureka moments” and have re-run the data with a new modified Basis Set that substantially improved their ability to accurately graph certain contaminant distribution via GIS, etc.